Hydrogen-induced sp^2-sp^3 rehybridization in epitaxial silicene

Dmytro Solonenko,[1,*] Volodymyr Dzhagan,[1] Seymur Cahangirov,[2] Cihan Bacaksiz,[3] Hasan Sahin,[4,5]
Dietrich R. T. Zahn,[1] and Patrick Vogt[1]

[1]*Semiconductor Physics, Chemnitz University of Technology, 09126 Chemnitz, Germany*

[2]*UNAM–National Nanotechnology Research Center and Institute of Materials Science and Nanotechnology,*
Bilkent University, 06800 Ankara, Turkey

[3]*Department of Physics, Izmir Institute of Technology, 35430 Izmir, Turkey*

[4]*Department of Photonics, Izmir Institute of Technology, 35430 Izmir, Turkey*

[5]*ICTP-ECAR Eurasian Center for Advanced Research, Izmir Institute of Technology, 35430, Izmir, Turkey*

We report on the hydrogenation of $(3 \times 3)/(4 \times 4)$ silicene epitaxially grown on Ag(111) studied by *in situ* Raman spectroscopy and state-of-the-art *ab initio* calculations. Our results demonstrate that hydrogenation of $(3 \times 3)/(4 \times 4)$ silicene leads to the formation of two different atomic structures which exhibit distinct spectral vibrational modes. Raman selection rules clearly show that the Si atoms undergo a rehybridization in both cases from a mixed sp^2-sp^3 to a dominating sp^3 state increasing the distance between the two silicene sublattices. This results in a softening of the in-plane and a stiffening of the out-of-plane phonon modes. Nevertheless, hydrogenated epitaxial silicene retains a two-dimensional nature and hence can be considered as epitaxial silicane. The level of hydrogenation can be determined by the intensity ratio of the Raman modes with different symmetries.

I. INTRODUCTION

The physical properties of epitaxial silicene on Ag(111) [1–3] differ from the properties predicted for its free-standing counterpart [4–6]. Both forms of silicene share a metallic nature [7] detrimental for their application in semiconductor technology. In order to retrieve a semiconducting character of silicene, i.e., open an electronic band gap and tune the electronic properties, surface adsorption could be a solution. Such functionalization was theoretically shown to alter the physical properties of free-standing silicene [8–10]. For example, hydrogenation can result in a band gap opening in the range of several eV [8]. Fully hydrogenated free-standing silicene, or silicane, exhibits a direct band gap of about 3 eV at the Γ point of the Brillouin zone [11]. This effect is evoked by covalently attached H atoms, which increase the distance between the two silicene sublattices and, hence, lead to a breaking of the π bonds [11–13].

Although hydrogenation of epitaxial silicene is experimentally feasible due to its high chemical reactivity [14], the experimental investigation of hydrogenated silicene are scarce, except studies by scanning tunneling microscopy (STM) [15,16] and high-resolution electron-energy-loss spectroscopy [16]. The reported STM images show that the atomic structure of hydrogenated epitaxial silicene [15,16] differ from the one expected for silicane, while hydrogen exposure results in a rearrangement of the silicene lattice in a predominantly ordered fashion, yielding the formation of so-called hydrogenated γ-silicene [15]. This γ phase has a unit cell based on the unit cell of $(3 \times 3)/(4 \times 4)$ silicene, where the buckling direction between the two triangular halves changes. As a result, in one half six Si atoms are up-buckled and saturated by H and in the other half only one Si atom is

up-buckled and saturated by H [see Fig. 3(d)] [15]. Such a reconstruction is only observed after hydrogenation. Due to the asymmetry of its unit cell, it loosely resembles another pristine silicene phase, a so-called β-silicene, which forms on Ag(111) and can be explained by three horizontal Si planes, separated by the buckling distance [17]. Besides the γ phase, another H-silicene phase is reported, where the unit cell is symmetrically hydrogenated, termed α-silicene [15,16]. In this phase, H adsorbs directly at the six up-buckled Si atoms of the symmetric $(3 \times 3)/(4 \times 4)$ unit cell [see Fig. 3(b)]. The appearance of α-silicene in STM is reported to be identical before and after hydrogenation, making its identification by STM troublesome. Moreover, important aspects of these epitaxial silicane-like layers, such as the hybridization state of the Si atoms, are not known. Similarly, it is not clear whether the two-dimensional (2D) vibrational character of epitaxial silicene is preserved during hydrogenation, i.e., the presence of in-plane and out-of-plane phonon modes.

In order to understand the structural change of pristine epitaxial silicene on hydrogenation, we perform *in situ* Raman spectroscopy study during the exposure of silicene to atomic hydrogen. *In situ* Raman studies were carried out for pristine epitaxial silicene on Ag(111) [18,19] and allowed to identify its spectral signature, exhibiting optical phonon bands at 175, 216, and $514 \, \text{cm}^{-1}$, with A- and E-type symmetries that underline the 2D character of epitaxial silicene layers [20]. The mode symmetries also helped to assign the bands to particular vibrations, paving the way for using the Raman data as a reference to study the functionalization of silicene *in situ*.

II. METHODS

Silicene samples are prepared under ultra-high vacuum (UHV) conditions ($P_{\text{base}} = 2 \times 10^{-10}$ mbar) via Si atoms adsorption on clean Ag(111) surfaces. The quality of the silver surface and 2D crystals deposited is verified by low-energy

_____

*dmytro.solonenko@physik.tu-chemnitz.de

electron diffraction at electron energies below 40 eV. The hydrogenation is performed via cracking the molecular hydrogen in the proximity (<3 cm) of the sample with a freshly grown silicene layer. Due to the fact that epitaxial silicene exhibits Raman signals, which are too low to be acquired during the time of hydrogenation, the monitoring of hydrogenation is performed in steps after which single spectra are acquired, each with a typical acquisition time of 144 s. Here one hydrogenation step corresponds to the 25-Langmuirs (L) exposure of silicene to atomic hydrogen (25-s exposure at 10^{-6} Torr of hydrogen partial pressure). Raman measurements are carried out *in situ* using a triple monochromator Dilor XY800 spectrometer and the 514.5-nm Ar$^+$ laser line as an excitation with a spectral resolution of 3.3 cm^{-1} and a power density below 10^3 W cm^{-2}.

Density functional theory (DFT) calculations are performed using a projector augmented wave method which is implemented in the Vienna *ab initio* Simulation Package [21–23]. To describe electron exchange and correlation, the Perdew-Burke-Ernzerhof form of the generalized gradient approximation is adopted [24]. Van der Waals interaction, important for layered materials, is taken into account by using the DFT-D2 method of Grimme [25]. The calculations are performed using the following parameters: a kinetic energy cut-off of 500 eV; a total energy difference between the sequential steps in the iterations of 10^{-5} eV units as a convergence criterion; a convergence for the Hellmann-Feynman forces per unit cell of 10^{-4} eV/Å; and a Gaussian smearing of 0.05 eV. $3 \times 3 \times 1$ Γ-centered k-point sampling is used for the Brillouin zone integration. To avoid vertical interactions in the stack, the calculations are performed with a vacuum spacing of ~ 10 Å. The Ag (111) surface is modelled by two truncated layers of Ag with respect to fcc Ag. Due to the perfect lattice matching of the (4×4) supercell of the Ag (111) surface and that of the (3×3) silicene, $(3 \times 3)/(4 \times 4)$ silicene/Ag (111) is taken as a unit cell during the calculations. The vibrational properties are calculated using the small-displacement method within the harmonic approximation which is implemented in the PHON code [26]. The phonon dispersions for the Si-H system are derived from the calculated force constants. The influence of the Ag template is implemented by calculating the forces on the Si and H atoms on their displacement in the (2×2) supercell of the $(3 \times 3)/(4 \times 4)$ silicene/Ag(111). The reduced mass effect is accounted for by multiplication of $\sqrt{1 + (m_{Si} + m_H)/m_{Ag}}$ to the obtained frequencies [20].

III. RESULTS AND DISCUSSION

Figure 1 shows the Raman spectra of epitaxial $(3 \times 3)/(4 \times 4)$ silicene during step-wise hydrogenation. The spectrum of the initial epitaxial silicene layer, recorded after Si deposition, fully reproduces our previous results [20]. It shows two A Raman modes (A^1 at 175 cm^{-1} and A^2 at 216 cm^{-1}), assigned to out-of-plane vibrations, and an E mode at 514 cm^{-1}, related to an in-plane lattice vibration, in excellent agreement with the selection rules of its C$_{6v}$ symmetry group [20,27]. The low-energy shoulder of the E mode originates from the coformation of the amorphous Si during the Si deposition. In the Supplemental Material we provide details on the treatment
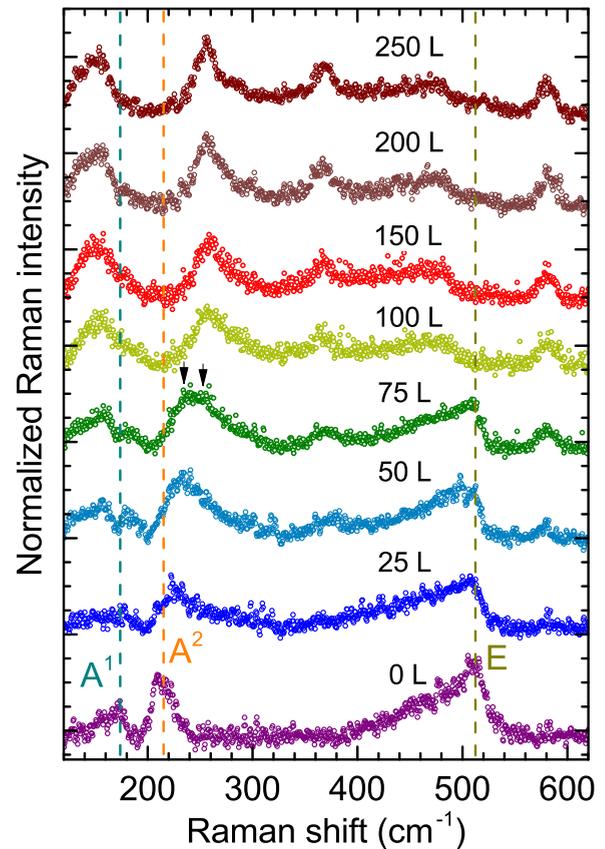
FIG. 1. Raman spectra of the epitaxial (3×3) silicene during step-wise hydrogenation. The hydrogenation is measured in Langmuirs (L), which denotes the dose of H exposure. The spectra are stacked for the clarity.

of the Raman signal of amorphous Si on hydrogenation [28]. At low hydrogen coverage (25 L), the relative intensities of the A^1 and E Raman modes decrease (Fig. 1). The A^2 mode, on the other hand, shifts towards higher energies by 4 cm^{-1} and broadens. For 50-L H exposures, the A^2 mode shifts to 236 cm^{-1} and becomes asymmetric. The asymmetry is due to a broad shoulder, centered around 275 cm^{-1}, which actually consists of several different contributions. In this case, it is difficult to discriminate between the former A^2 mode and other modes possibly formed due to hydrogenation. However, we can assume that the resulting Raman band at 258 cm^{-1} after H exposure of 100 L originates from the former A^2 Raman mode. Around the position of the disappearing A^1 mode, we observe the appearance of a broad band. New Raman bands also emerge around 369 cm^{-1} and 585 cm^{-1}. The intensity of the E mode gradually decreases, indicating a significant rearrangement of the silicene lattice on hydrogenation. It can be noticed that the spectral modifications cease at a dose of 100 L. The positions and relative intensities of the distinct Raman bands at 147, 258, 369, and 585 cm^{-1} remain unaltered with further hydrogen exposure. Hence, at a dose of 100-L saturation of the hydrogenation is reached.

The evolution of the Raman spectra of epitaxial silicene on hydrogenation indicates a lattice rearrangement due to a chemisorption of the H atoms. A substantial change of
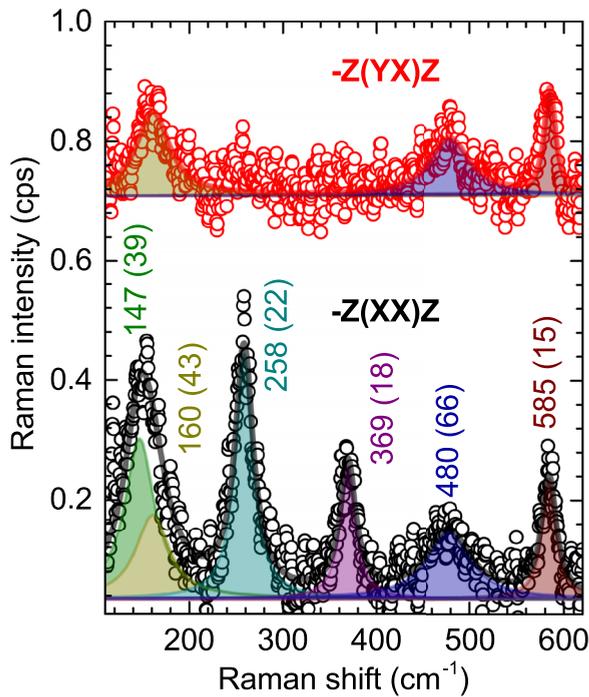
FIG. 2. Polarization-dependent Raman spectra of hydrogenated silicene (250-L dose) in parallel [-z(xx)z] and crossed [-z(yx)z] geometries. The Raman bands are marked with their positions and the full widths at half maximum are shown in parenthesis.

the mode characteristics is observed for the A^2 mode. Its frequency shift can be understood in terms of the vibrational patterns. According to the mode assignment [20], the A modes correspond to an out-of-plane atomic motion of the Si atoms in the 2D lattice and differ by their phase and the contribution of oppositely buckled Si atoms in the motion. The A^1 mode corresponds to the in-phase motion of Si atoms with larger eigenvectors of the down-buckled Si atoms, while the A^2 mode represents the out-of-phase atomic motion of the up-buckled Si atoms. Hence, we can assume that the shift of the out-of-phase A^2 mode towards higher energies is caused by a stiffening of the silicene lattice, which is a result of the restriction of the Si atoms motion by the adsorbed H atoms orthogonal to the lattice plane. Although the hydrogen atoms have a small mass, their number per unit cell (up to 7 H atoms, in the case of γ-silicene) and the lattice symmetry change have a major impact on the lattice vibrations. Remarkably, at the same time, the in-phase A^1 mode disappears on hydrogenation, indicating a damping of the out-of-plane motion of the down-buckled Si atoms. The apparent broadening of the A^2 mode can be explained by the spectral band asymmetry, which originates from the overlap of this band and the one of amorphous silicon.

The Raman band symmetry can be retrieved by polarization-dependent measurements, performed in parallel and crossed geometries [in Porto notations: -z(xx)z and -z(yx)z, respectively]. Here the x and y axes lie in the plane of the silicene layer, while the z axis is perpendicular to the 2D layer. In Fig. 2 it is shown that the Raman spectrum, recorded in parallel scattering configuration, exhibits six Raman bands, while in the crossed configuration only three Raman bands are seen. These clear selection rules indicate a

high crystalline order of the hydrogenated layer. According to STM measurements reported by Qiu *et al.* [15], the symmetry of the silicene lattice after hydrogenation is reduced from hexagonal to trigonal. In this case, the point symmetry group in the case of γ-silicene is C_{3v}, which is determined from its Wigner-Seitz cell. The Raman tensors of the C_{3v} group are of A and E type, similarly to the ones of the C_{6v} group. The the absence of Raman bands at 147, 258, and 369 cm^{-1} in crossed scattering configuration allows them to be attributed to A modes. On the other hand, E modes should be observed in both geometries as found for the bands at 160, 480, and 585 cm^{-1}.

The origin of the mode at 585 cm^{-1} is especially interesting because it coincides with the position of the L(T)O mode of free-standing silicene [6]. However, the formation of free-standing silicene by intercalation of H and associated weakening of the silicene-substrate interaction is unlikely. It is known that the hydrogen atoms adsorb on the top of the silicene lattice [15]. Moreover, such vibrational frequencies can also be found in similar Si systems, such as polysilanes [29,30] (Si-H bending at 643.8 cm^{-1} and Si-H rocking at 630 cm^{-1}) and hydrogen passivated bulk Si [31]. These Si vibrations are induced by the presence of hydrogen and thus cannot be found in pure Si systems. Together with the Raman selection rules, it shows that hydrogenated epitaxial silicene, or epitaxial silicane, consists of a two-dimensional Si layer and the H atoms. This material exhibits a 2D character despite the dominant sp^3 hybridization of the Si atoms, which is possible when a non-negligible substrate-adlayer interaction is considered [7].

The substantial silicene-Ag interaction can also be inferred from the softening of the E mode of epitaxial silicene from 514 cm^{-1} to 480 cm^{-1}, which is consistent with the concept of the rehybridization of the Si atoms and implies that the Si-Si bond length must be enlarged as a result of a bond energy reduction. This bond weakening is caused by the hydrogen adsorption which rearranges the electron distribution in neighboring Si-Si bonds. Our Bader charge analysis shows that, on average, 0.5 electrons are transferred from the Si atoms to the H atoms during the Si-H bond formation. The energy reduction results in a redshift of the E mode of epitaxial silicene. This exemplifies the sp^2-to-sp^3 transition observed as a result of the hydrogen adsorption and the related rehybridization. In the case of free-standing silicane [11], the silicene sublattices should be more separated as compared to free-standing silicene. Our DFT calculations reveal that the distance between the planes of up- and down-buckled Si atoms is enlarged by 0.1 Å for hydrogenated α-silicene and by 0.16 Å for hydrogenated γ-silicene. The angle between the planes is increased by 2° and 4.1°, respectively, while the Si-Si bond angles are decreased at the same time. In the Supplemental Material we show a detailed information on the angles and distances in hydrogenated silicene phases [32]. These results confirm that the H-adsorption causes an increase of the sublattice distance in epitaxial silicene on Ag(111). For free-standing silicene, such an increased separation leads to a band gap opening, which is not observed here as a result of the non-negligible interaction with the substrate. However, the results show that if the substrate interaction is reduced (e.g., by choosing different substrate materials or
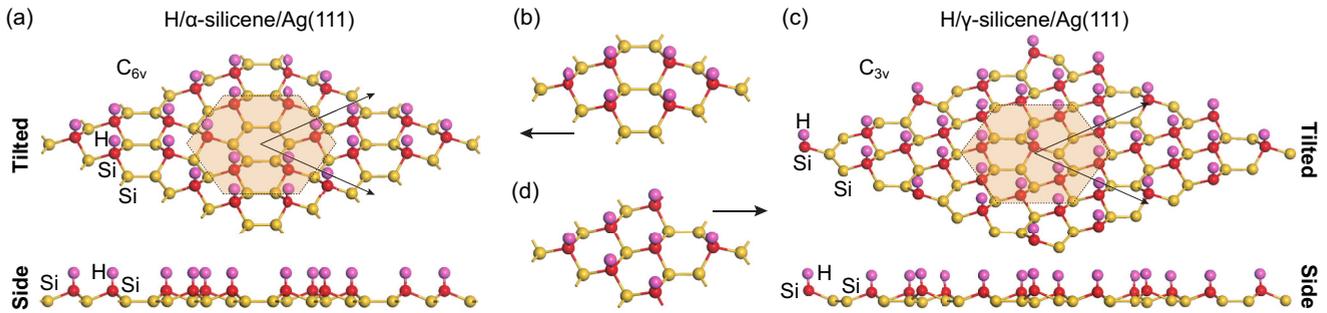
FIG. 3. Tilted and side views of the ball-and-stick model of hydrogenated (a) α- and (c) γ-silicene. The atoms of the underlying Ag(111) substrate are not shown. The shaded hexagonal region corresponds to the Wigner-Seitz unit cell of the system. The (3×3) supercells of hydrogenated (b) α- and (d) γ-silicene are shown separately.

intercalation) H-absorption is likely to cause the opening of an electronic band gap of epitaxial silicene. This band also exhibits a large linewidth, which can be related to the fact that softening of the in-plane phonon vibrations in α- and γ-silicenes should occur differently due to their structural distinction. This can lead to several phonon contributions to this spectral band, making it apparently broader. Last, the other E mode of hydrogenated epitaxial silicene at 160 cm^{-1} has no straightforward experimental assignment, since it has no equivalent in the Raman spectrum of pristine epitaxial silicene. Therefore, we use the simulated phonon dispersions to assign this mode to an Si-Si in-phase out-of-plane motion.

The calculated atomic arrangement of hydrogenated α- and γ-silicene are shown in Fig. 3. The H atoms are bonded to the up-buckled Si atoms despite the underlying Si lattice. The number of the up-buckled Si atoms in the α-silicene structure is similar to the one of the $(3 \times 3)/(4 \times 4)$ Si superstructure. In the case of γ-silicene there are seven up-buckled Si atoms in agreement with STM observations [15]. The phonon dispersions, calculated in the first Brillouin zone of α- and γ-silicene phases are shown in Fig. 4. Due to the substrate-originated reconstructed structure of silicene, the number of phonon branches reaches 72 for both structures. Obviously, not all calculated vibrational modes are observed in the experiment. First, the overall Raman intensity might be too low to observe all allowed vibrations and only intense ones are seen. The mode spectral activity also decreases if the mode is both Raman and IR active. Second, we use only one experimental scattering configuration and therefore not all phonons are probed by Raman spectroscopy. According to the symmetry group considerations, in the back-scattering geometry with the light propagating along the z axis, only the A_1(LO) and E(TO) modes are allowed for the γ phase, while the A_1(TO) and E(LO) ones are forbidden. For the α phase, only the A_1(LO) and E_2 modes are allowed and the A_1(TO) and E_1(TO) modes are forbidden. Obviously, the forbidden modes become allowed when the light (either incident, or scattered) propagates in the plane of the crystal, which is, however, experimentally vague in the case of 2D materials. Hence, in order to assign the experimental Raman bands, we need to compare both the calculated phonon energy at the Γ point and the phonon symmetry.

The γ-silicene phase has phonon modes that match the energies of the bands observed experimentally for hydrogenated epitaxial $(3 \times 3)/(4 \times 4)$ silicene: two A modes at 149.8 and

368.0 cm^{-1} and three E modes at 161, 477, and 584 cm^{-1} at the Γ point. The only spectral band, not found in the calculations is the A mode at 258 cm^{-1}. Clearly, the γ-silicene phase exhibits no vibration of close frequency [Fig. 4(b)]. The nearest phonon mode is located at 283 cm^{-1}, which is too far and must have another origin, for example, belonging to the coexisting silicene phase [17]. In the phonon dispersion for hydrogenated α-silicene [Fig. 4(a)], a phonon mode of A symmetry at 247.3 cm^{-1} at Γ is present, which is clearly close to the experimental A mode at 258 cm^{-1}. Therefore, we assume that this Raman band indicates the presence of the hydrogenated α-silicene phase. The other Raman-active vibrations of this phase, in particular E modes at 469.6 and 583.2 cm^{-1}, overlap with the E modes of γ-silicene, while all other A modes except the one at 247.3 cm^{-1} presumably have low Raman intensity and, therefore, are not detected. Hence, we conclude that the Raman bands of A symmetry at 147 and 369 cm^{-1} are the spectral markers of γ-silicene and the Raman band of A symmetry at 258 cm^{-1} is the marker of α-silicene. This is also reflected in a recent HREELS study, which reports the vibrational mode at 597 cm^{-1}, the spectral position of which resembles the Raman-active E mode at 585 cm^{-1} [16]. Its assignment to the Si-H bending agrees with our calculations. Although, the mechanism of hydrogenation is far from clear, the multiphase formation on hydrogen adsorption may originate from the sample irregularities such as domain boundaries. Their metastability in epitaxial silicene was demonstrated in a recent STM study [33]. Therefore, it is possible to assume that silicene domains and their boundaries will differently respond to the hydrogen adsorption, which can eventually result in a formation of two phases. Based on the DFT calculations, we can now assign the experimental bands to certain vibration patterns of hydrogenated epitaxial silicene for selected phonon modes of γ- and α-silicene [34]. Accordingly, the A modes at 149.8 and 368.0 cm^{-1} are assigned to out-of-plane lattice vibrations, i.e., Si-H stretching modes. The phonon mode at 160 cm^{-1} has also an out-of-plane motion character; however, the Si and H atoms move in-phase either away from or to the substrate with a minor contribution of lateral motion. On the contrary, the E mode at 477.1 cm^{-1} includes only lateral motion of the Si and H atoms. The motion of the Si atoms is identical to the pattern of the E mode of pristine epitaxial silicene on Ag(111) [20], which confirms their similarity. Last, the E band at 585 cm^{-1}, which corresponds to a normal mode with a frequency of 584.5 cm^{-1}, has a clear assignment to the
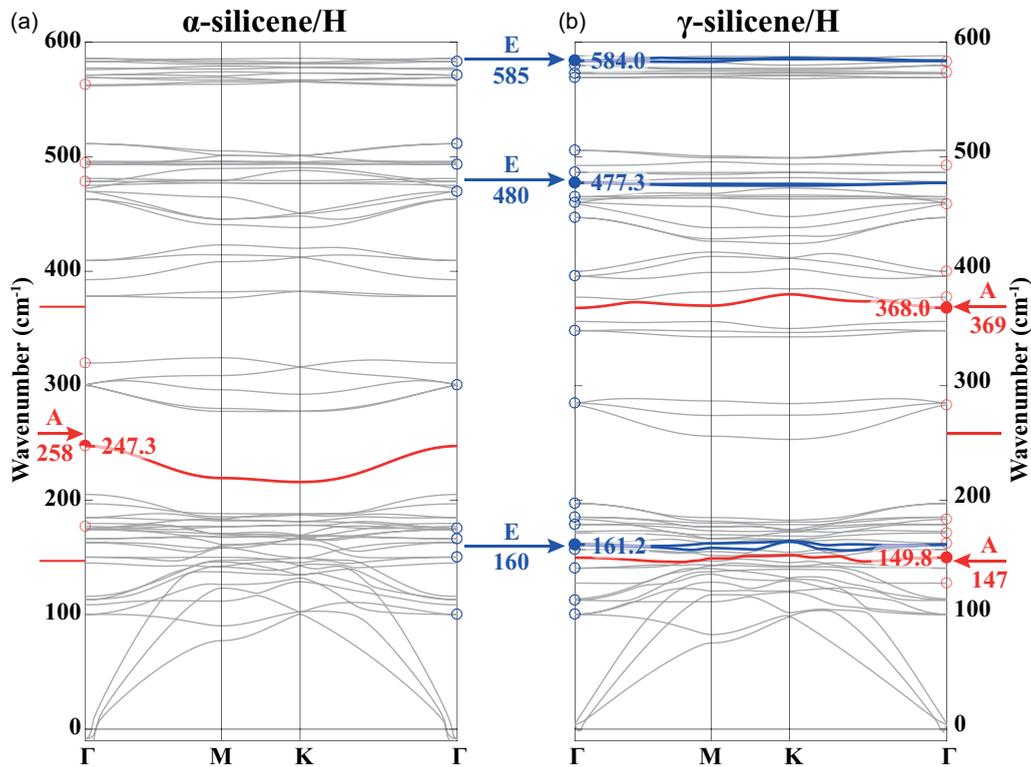
FIG. 4. Phonon dispersions of hydrogenated α- (a) and γ-silicene (b) on Ag(111) substrate. The experimentally detected A and E modes are denoted by the red and the blue arrows, respectively. The measured frequency is written underneath in cm^{-1} units. The calculated Raman active A and E modes are shown by the red and the blue circles, respectively. The Raman active modes assigned to the experimental values are shown by the filled circles and the calculated wave numbers are written next to them. The assignment of the A mode measured at 258 cm^{-1} is shown by the half-filled circle since the calculated value is 11 cm^{-1} lower.

Si-H bending vibration. According to the eigenvector sketch, the Si atoms are suspended while the H atoms loosely move around their equilibrium positions. As mentioned above, the A symmetry lattice vibration with a frequency of 283 cm^{-1} is not observed in the Raman spectra. However, its vibrational pattern is identical to the one, which corresponds to the Raman mode at 258 cm^{-1}. This nicely shows that the same lattice vibrations can have different energies in the case of the different structural phases and, therefore, can be used to distinguish one from another. However, the reason for their distinct spectral activity is not clear. This Raman mode is assigned to the Si-Si twisting vibration.

Despite the fact that the underlying mechanism of the hydrogenation of epitaxial silicene is not fully understood yet, our Raman results suggest that it can be described quantitatively. The level of the silicene hydrogenation can be determined by the ratio of the spectral bands with different symmetries. Figure 5 shows the ratio of the A mode at 258 cm^{-1} to the E mode at 585 cm^{-1} as a function of H exposure. This ratio is highly sensitive to the small H doses and thus the experimental points can be fitted with an exponential curve. The computational analysis reveals a Si-H binding energy of 2.6 eV. In the case of a monomolecular adsorption, such process is self-limiting, which is in agreement with the experimental observation of a H saturation at 100 L, which corresponds to a ratio value around 3.8. This mode ratio does not depend on sample parameters and can be used for determination of the hydrogenation level.

Last, the photoluminescence (PL) spectra of the hydrogenated silicene, measured with the same experimental setup, do not show PL bands between 1.5 and 2.4 eV, which is in agreement with our DFT calculations of the band structure of α- and γ-silicene. The simulations suggest a metallic character for both phases, in contrast to the expectations of a band gap opening for silicane [11]. The absence of a PL band in the visible spectral range confirms the theoretical predictions. This
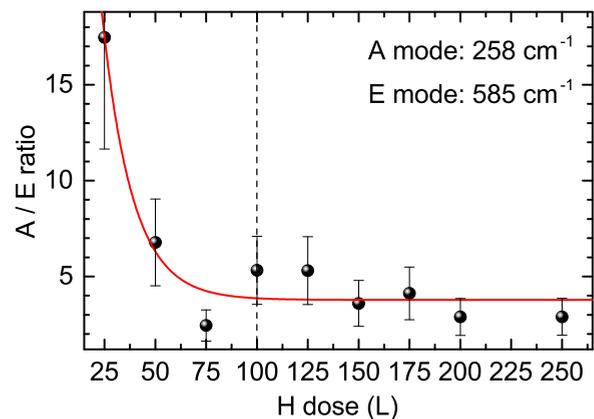
FIG. 5. Integral intensity ratio between A and E modes at 258 and 585 cm^{-1}, respectively, as a function of the atomic hydrogen exposure. The error bars were determined from the fit.

points out the epitaxial nature of epitaxial silicane, a 2D Si-H material on Ag(111).

IV. CONCLUSION

In summary, we applied *in situ* Raman spectroscopy and *ab initio* calculations to study the hydrogenation of epitaxial $(3 \times 3)/(4 \times 4)$ silicene on Ag(111). We find that hydrogenation leads to a structural modifications of silicene observed by a drastic change of its vibrational properties. Hydrogenated silicene exhibits six sharp Raman bands which are assigned to α- and γ-silicene phases. Their formation is attributed to the sample irregularities, such as domain boundaries. The determined mode symmetries show that hydrogenated epitaxial silicene retains a two-dimensional character. The evolution of its spectral signature on hydrogenation and the DFT calculations indicate a rehybridization of the Si atoms and thus a buckling enhancement. Such a result suggests that hydrogen adsorption partially weakens the substrate-adlayer interaction which can be interpreted as the formation of epitaxial silicane, distinct from other hydrosilicon-like systems. The degree of hydrogenation can be determined from the ratio between the Raman bands of different symmetries. Our results demonstrate that hydrogenation of epitaxial silicene leads to an increase of the sublattice distance, which is important for the investigations of epitaxial silicane, which may find place in hydrogen-storage applications.

[1] P. Vogt, P. De Padova, C. Quaresima, J. Avila, E. Frantzeskakis, M. C. Asensio, A. Resta, B. Ealet, and G. Le Lay, Phys. Rev. Lett. **108**, 155501 (2012).

[2] C.-L. Lin, R. Arafune, K. Kawahara, N. Tsukahara, E. Minamitani, Y. Kim, N. Takagi, and M. Kawai, Appl. Phys. Express **5**, 045802 (2012).

[3] B. Feng, Z. Ding, S. Meng, Y. Yao, X. He, P. Cheng, L. Chen, and K. Wu, Nano Lett. **12**, 3507 (2012).

[4] K. Takeda and K. Shiraishi, Phys. Rev. B **50**, 14916 (1994).

[5] G. G. Guzmán-Verri and L. C. L. Y. Voon, Phys. Rev. B **76**, 075131 (2007).

[6] S. Cahangirov, M. Topsakal, E. Akturk, H. Şahin, and S. Ciraci, Phys. Rev. Lett. **102**, 236804 (2009).

[7] S. Cahangirov, M. Audiffred, P. Tang, A. Iacomino, W. Duan, G. Merino, and A. Rubio, Phys. Rev. B **88**, 035432 (2013).

[8] L. C. L. Y. Voon, E. Sandberg, R. S. Aga, and A. A. Farajian, Appl. Phys. Lett. **97**, 163114 (2010).

[9] J. Sivek, H. Sahin, B. Partoens, and F. M. Peeters, Phys. Rev. B **87**, 085444 (2013).

[10] B. Huang, H. J. Xiang, and S.-H. Wei, Phys. Rev. Lett. **111**, 145502 (2013).

[11] V. Zolyomi, J. R. Wallbank, and V. I. Fal'ko, 2D Mater. **1**, 011005 (2014).

[12] T. H. Osborn, A. A. Farajian, O. V. Pupysheva, R. S. Aga, and L. C. L. Y. Voon, Chem. Phys. Lett. **511**, 101 (2011).

[13] P. Zhang, X. D. Li, C. H. Hu, S. Q. Wu, and Z. Z. Zhu, Phys. Lett. A **376**, 1230 (2012).

[14] S.-Y. Lin, S.-L. Chang, N. T. T. Tran, P.-H. Yang, and M.-F. Lin, Phys. Chem. Chem. Phys. **17**, 26443 (2015).

[15] J. Qiu, H. Fu, Y. Xu, A. I. Oreshkin, T. Shao, H. Li, S. Meng, L. Chen, and K. Wu, Phys. Rev. Lett. **114**, 126101 (2015).

[16] D. B. Medina, E. Salomon, G. L. Lay, and T. Angot, J. Electron Spectrosc. Relat. Phenom. **219**, 57 (2017).

[17] Z.-L. Liu, M.-X. Wang, J.-P. Xu, J.-F. Ge, G. L. Lay, P. Vogt, D. Qian, C.-L. Gao, C. Liu, and J.-F. Jia, New J. Phys. **16**, 075006 (2014).

[18] J. Zhuang, X. Xu, Y. Du, K. Wu, L. Chen, W. Hao, J. Wang, W. K. Yeoh, X. Wang, and S. X. Dou, Phys. Rev. B **91**, 161409(R) (2015).

[19] A. D. Alvarez, T. Zhu, J. P. Nys, M. Berthe, M. Empis, J. Schreiber, B. Grandidier, and T. Xu, Surf. Sci. **653**, 92 (2016).

[20] D. Solonenko, O. D. Gordan, G. L. Lay, H. Sahin, S. Cahangirov, D. R. T. Zahn, and Patrick Vogt, 2D Mater. **4**, 015008 (2017).

[21] G. Kresse and J. Hafner, Phys. Rev. B **47**, 558(R) (1993).

[22] G. Kresse and J. Furthmuller, Phys. Rev. B **54**, 11169 (1996).

[23] G. Kresse and D. Joubert, Phys. Rev. B **59**, 1758 (1999).

[24] J. P. Perdew, K. Burke, and M. Ernzerhof, Phys. Rev. Lett. **77**, 3865 (1996).

[25] S. Grimme, J. Comput. Chem. **27**, 1787 (2006).

[26] D. Alfe, Comput. Phys. Commun. **180**, 2622 (2009).

[27] D. Solonenko, O. D. Gordan, G. L. Lay, D. R. T. Zahn, and P. Vogt, Beilstein J. Nanotechnol. **8**, 1357 (2017).

[28] See Supplemental Material at http://link.aps.org/supplemental/10.1103/PhysRevB.96.235423 for the discussion on the signal of amorphous Si, coformed with epitaxial silicene on hydrogenation.

[29] P. Vora, S. A. Solin, and P. John, Phys. Rev. B **29**, 3423 (1984).

[30] Y. Kumai, S. Shirai, E. Sudo, J. Seki, H. Okamoto, Y. Sugiyama, and H. Nakano, J. Power Sources **196**, 1503 (2011).

[31] M. Cardona, Phys. Status Solidi (b) **118**, 463 (1983).

[32] See Supplemental Material at http://link.aps.org/supplemental/10.1103/PhysRevB.96.235423 for the detailed structural information obtained by DFT simulations.

[33] Y. Oh, Y. Cho, H. Kwon, J. Lee, I. Jeon, W. Ko, H. W. Kim, J. Ku, G. Kim, H. Suh *et al.*, Appl. Phys. Lett. **110**, 263112 (2017).

[34] See Supplemental Material at http://link.aps.org/supplemental/10.1103/PhysRevB.96.235423 for the vibrational motion patterns of α and γ phases of epitaxial silicane.